Astronomy & Astrophysics manuscript no. asters2
September 29, 2008

Discovery of the binary nature of the Mars–crosser (1139) Atami ⋆

R. Behrend[1,26], F. Manzini[2], A. Klotz[3,4], F. Colas[5,6], Y. Damerdji[3,4], S. J. Ostro[7], P. Antonini[8,6], E. Barbotin[6], L. A. M. Benner[7], L. Bernasconi[9,6], C. Cavadore[6], S. Charbonnel[10,6], J. Coloma[11], R. Crippa[2], G. Farroni[12], R. Koff[13], F. Kugel[14], J. D. Giorgini[7], A. A. Hine[15], A. Leroy[16], J.-M. Llapasset[17], C. Magri[18], J.-L. Margot[19], M. C. Nolan[15], A. Oksanen[20], P. Pääkkönen[21], R. Poncy[22,6], R. Roy[23,6], D. Starkey[24], H. Correia[25], and D. Paletti[25]

(Affiliations can be found after the references)

Received September 29, 2008 /Accepted

ABSTRACT

Context. Asteroids with satellites are useful to probe the dynamical evolution of the solar system.
Aims. The minor planet (1139) Atami exhibited mutual eclipses on its light curve during the 2005 opposition. We used these events to study the binary nature of this Mars–crossing asteroid.
Methods. We used geometric methods applied to photometric data and Doppler-resolved radar echoes to deduce orbital and physical characteristics of the two bodies.
Results. We assume that (1139) Atami is a double body system composed by two prolate ellipsoids (of size $2r_a \times 2r_b \times 2r_b$) with the same axial ratio r_b/r_a. From photometric light curves, the major–axes should point each other implying that rotation and revolution are synchronous with a period $T = 1.14361 \pm 0.00023$ day. **According to the model taken in this study, photometric and radar data analysis reveal that r_b/r_a=0.65 ±0.02 and a circular orbit with a center-to-center separation of $s = 17.56 \pm 1.48$ km. From the duration of the eclipse features of the light curve, we derive the bulk density $\rho = 2.6 \pm 0.5$ g/cm^3, and the pole orientation: $\lambda_p = 264 \pm 5°$, $\beta_p = +5 \pm 5°$. The intensity of radar echoes implies that the body dimension ratio is 0.82 ±0.08. The bulk density is very sensitive to the eclipse duration. As we observed a fast evolution of the eclipse features, this value must be refined during the next oppositions (next observable eclipses are predicted in 2009). Spectrometry and BVRI photometry performed during eclipses reveal that the two bodies have the same reflectance properties and are probably members of the S spectral class. Radar albedo and archived spectroscopic observations show that the surface nature is probably moderatly rough at decimetre scales.**
Conclusions.

Key words. Planets: formation – Asteroids: binary systems – Techniques: photometry – Techniques: radar

1. Introduction

Certain binary asteroids are composed by two bodies of almost the same sizes. Such systems are already known in the main belt (*e.g.* Merline et al. 2000, Behrend et al. 2006), in the Trojan family (Merline et al. 2001), in the Kuiper belt (*e.g.* Veillet et al. 2002), and among Near Earth Asteroids (*e.g.* Pravec & Hahn 1997, Margot et al. 2003). In the case of Mars–crossers, at the time of the discovery of Atami's binarity, only (5407) 1992 AX was suspected to have a secondary as large as 30% of the size of the primary (Pravec et al. 2000). Other Mars–crossers were found to be binaries: (2044) Wirt (Pray et al., 2006), (34706) 2001 OP83 (Warner et al., 2005; Goncalves et al., 2005), (114319) 2002 XD58, (Pray et al., 2006).

Migliorini et al. (1998) and Michel et al. (2000) studied the dynamical stability of Mars–crossers and found a median life time of about 60 Myr. These studies concluded that the Mars–crossing population could be the main intermediate reservoir of multikilometer Earth–crossing asteroids. Many resonances of Mars, Jupiter and Saturn in the groups Hungaria and Phocaea families and in other parts of the main belt induce chaotic diffusions that can enrich continuously the Mars–crosser population.

The orbital elements of Atami ($a = 1.947$ AU, $i = 13.1°$) are compatible with the EV (*evolved*) group of Mars–crossers ($1.77 < a < 2.06$ AU and $i < 15°$) defined by Michel et al. (2000). They describe this group as a rather stable region (median life time of about 100 Myr) which is enriched mainly by the Hungaria group and have exchanges with the Earth–crossing group. Early photometric measurements of Atami, reported by Lupishko et al. (1988), indicated a period longer than 20 hours and a total amplitude of greater than 0.18 magnitude. The reflectance spectrum obtained on 1996 Apr. 29 by Bus & Binzel (2002a) suggests an S–type. Another series of spectra taken in 1997 Dec. 21-26 by Angeli & Lazzaro (2002) suggest a C–type. These discrepancies were noticed but not explained by the authors.

This paper is devoted to the discovery and characetrization of the binary nature of Atami. We explain the observational methods used for the determination of the dimensions and orientation of the system of two components. We recorded spectra when the system was eclipsed and modeled the surface differences of the two bodies. We suggest this double body is the result of gravitational reaccumulation of a fragments from a parent body destroyed by a huge collision as described in Michel et al. (2001).

Send offprint requests to: Raoul Behrend, Raoul.Behrend@Obs.UniGe.CH

⋆ Based on observations performed with the T1M at the Pic du Midi, TAROT at the Calern observatory, T193cm, T80cm and T120cm at the Observatoire de Haute-Provence, Arecibo Observatory and by many amateur observatories coordinated by Geneva Observatory.

2. Observations and processing

2.1. Photometry

The techniques we used for detection of binary asteroids from light curves are fully described in Behrend et al. (2006). Our strategy consists of performing photometry continuously during a few hours on each of many asteroids. This follow-up is done by a group of amateurs of astronomy supervised by R. Behrend. The telescopes used have diameters in the range of 20 to 60 cm. In spite of their small apertures, these telescopes are usually used without filters and yield 0.05 mag dispersion for minor planets brighter than $R = 14$. Observers process their own images and extract differential magnitudes. Then the data are merged and analysed at Geneva Observatory (for details see Behrend et al. 2006). When the orbital plane of a binary asteroid in seen edge–on from Earth, the light curve exhibits two components: the rotational light curve and the eclipsing light curve. The first component is usually quasi-sinusoidal with an amplitude Δm. The second component is flat outside eclipses, and shows V-shape features of duration $\Delta\Phi$ (relative to the orbital period) and depths of Δe magnitude. Rapid data analysis alerts observers to concentrate their efforts on new suspected binaries. This was the case at the beginning of 2005 September when a V–shape feature was detected in a light curve obtained by Federico Manzini (Manzini et al. 2006). We noticed dramatic changes during 2005 Sep.: eclipses completely vanished at the end of the month. We report the light curve of Atami in Fig. 1 from all observer data and corresponding derived values in Table 1 modified as described in section 3.3.

We used the 120 cm telescope at the Observatoire de Haute–Provence (hereafter OHP-T120) and TAROT at the Calern Observatory (see a description in Klotz et al. 2005) to perform filtered photometry. Results are presented in the Table 2. For OHP-T120, we indicate a total error +/-0.05 which corresponds to the mean errors of reference stars during the nights. At the beginning of the night, the airmass was rather high that produces such an error. For the 0.25-m aperture telescope TAROT, the $1.8^\circ \times 1.8^\circ$ images were calibrated using only the bright TYCHO2 stars - to avoid a systematic shift in magnitude present for the faint stars -, and the transformations to standard bands given in Høg et al. 2000. No significant colour variations were detected, even during eclipses. According to the H conventional definition, we have to measure the mean magnitude outside eclipses. The observed ligh curve (see fig.4) shows that outside eclipses, the magnitude follows a sinusoidal behaviour that depends on the rotational phase Φ. We defined $\Phi = 0$ and $\Phi = 0.5$ at eclipses which is also the minima of light of the sinunoidal component. Maxima of the sinusoidal component occur at $\Phi = 0.25$ and $\Phi = 0.75$. During a period, we have four instants corresponding to the mean sinusoid value: $\Phi = 0.125$, 0.375, 0.675 and 0.875. In the Table 2, we indicate at which phase the mean magnitude was measured. Assuming the standard value $G = 0.15$, we find $H = 12.90 \pm 0.08$ (the error comes from the dispersion of the four values of the Table 2). We do not have enough phase angle dispersion to constraint G. So the H value can also be affected by a different G value. Our H value is slightly fainter than the value, 12.51 found in the Minor Planet Center data base (MPC 17261), even if we assume the extreme case $G = 0$ for our data. This discrepancy can be explained by the fact that we estimated the V-magnitude in our data as the mean value of the pure rotational component of the light curve which had $\Delta m \simeq 0.4$ magnitude during 2005 September.

Table 1. Observational parameters of Atami.

Date of radar observations	2005-10-29.1
Orbit plane inclination ψ	18°
Date of photometric observations	2005-09-01.0
Phase angle φ	26°
Synodic period T (hours)	27.4466 ±0.0055
Rotational amplitude Δm (mag)	0.476 ±0.02
Eclipsing amplitude Δe (mag)	0.75 ±0.03
Eclipsing duration $\Delta\Phi$ (phase)	0.0812 ±0.006

2.2. Spectrometry

We used two spectrographs at the Observatoire de Haute–Provence to measure the surface reflectance of the binary system during mutual eclipses. With the T193 telescope, we used CARELEC (Lemaitre et al. 1990) with a resolution of $R = 900$ (1.8 Å/pixel) in the range 4000–7600 Å. Exposure times were 900 s. At the T80 telescope, we used a new low resolution spectrograph with a resolution of $R = 150$ (15 Å/pixel) in the range 5800–7800 Å. In both cases, spectra are normalized by the star SAO 53622 of spectral type G2V. Fig. 3 top shows Atami's reflectance on 2005 Sep. 02.072 at the phase $\Phi = 0.95$. This phase corresponds to the date just before the beginning of the eclipse when both bodies contribute to the spectrum. Fig. 3 bottom is the ratio of a spectrum taken at $\Phi = 0.00$ (2005 Sep. 02.126, during total eclipse) to another one taken at $\Phi = 0.95$ (just before eclipse). Variations are less than 3% between 4500 and 7500 Å. Even if the body seen at $\Phi = 0.00$ is slightly bluer, the asteroid lies within the S–type limits. T80 spectra were taken during $\Phi = 0.00$ of 2005 Sep. 10.1 and also suggest an S–type.

2.3. Radar

We used the Arecibo S-band (2380-MHz, 12.6-cm) radar to obtain echo spectra (Doppler-only images) of Atami. Figure 2 shows echoes received in the same sense of circular polarization as transmitted (the SC sense) and the opposite (OC) sense. A circularly polarized wave is reversed upon normal reflection from a smooth dielectric surface, so the OC echo dominates if the surface looks smooth comparable to the radar wavelength. The figure shows the sum of echoes from five transmit-receive cycles (runs) over 1.5 hour centered on 2005 Oct. 29.104. This epoch corresponds to a phase $\Phi = 0.25$. The two separated peaks are the expected signature from a binary system with the components rotating in synchronism with their relative orbital motion, seen at an orbital phase with the line connecting the components closer to the plane of the sky than to the plane containing the line of sight and the orbit pole (0 Hz corresponds to the centre of mass as computed from the ephemerides. The one-sigma uncertainty in the Doppler ephemeris prediction for Atami's center of mass is 0.13 Hz, or about 1/7 of our frequency resolution). The negative-Doppler peak reaches 4 sigma at $\nu_2 = -11$ Hz and has a 2-sigma–crossing bandwidth of $\delta\nu_2 = 4$ Hz. The positive-Doppler peak reaches 6 sigma at $\nu_1 = 6$ Hz and has 2 sigma–crossing bandwidth of $\delta\nu_1 = 7$ Hz. The uncertainty assigned to peak frequencies and widths is ±1 Hz. The separation between the two peaks **is** $\Delta\nu = 17 \pm 1.4$ **Hz**. Atami's circular polarization ratio, $\mu_C = \sigma_{SC}/\sigma_{OC} = 0.4 \pm 0.2$, indicates a mild to moderate degree of surface roughness more typical of a near-Earth asteroid than a main belt asteroid. Our estimate of Atami's OC radar cross section is $\sigma = 5.5 \pm 1.4\,\mathrm{km}^2$.

Table 2. Colour indices of Atami. Φ range column indicates limits of the phases observed. Φ_H column displays the phase when the magnitude is measured for the H determination (see column magnitude). φ is the phase angle Sun-Atami-Earth.

Date	Φ range	Φ_H	B-V	V-R	V-I	φ	magnitude	reference
							H=12.51 ±0.02	MPC 17261
1989			0.92 ±0.02			7.94		Tedesco et al. 1989
29 Apr. 1996						7.2	V=15.8	Bus & Binzel (2002a)
01.99 Sep. 2005	0.75 - 0.88	0.875	0.91 ±0.06	0.53 ±0.06		26.5	V=14.65 ±0.02	TAROT
12.01 Sep. 2005	0.55 - 0.77	0.625	0.90 ±0.01	0.52 ±0.02	0.93 ±0.01	22.4	V=14.08 ±0.05	OHP-T120
12.84 Sep. 2005	0.35 - 0.66	0.375			0.97 ±0.03	22.0	V=14.10 ±0.05	OHP-T120
14.00 Sep. 2005	0.24 - 0.54	0.375	0.88 ±0.02	0.58 ±0.02	0.97 ±0.03	21.5	V=14.12 ±0.05	OHP-T120

3. Analysis

Given our spectra and filtered photometry, we assume the surface composition is the same for the two bodies. Some physical parameters can be extracted from the light–curve and radar echoes. In the first model we used, we assume the same sizes for the two bodies. This allows us deriving a range of sizes and the pole orientation. In a second model elaborated for the refinement of parameters, we adopt different component sizes extracted from the radar observations.

3.1. Model 1: two twin bodies

We modeled Atami as two prolate ellipsoids of same size ($2r_a \times 2r_b \times 2r_b$) with their longest axes pointing toward each other. This figure is predicted for tidal interactions of two close bodies (Danby 1992).

We assumed spin-orbit synchronism with circular orbits and period T. The center-to-center separation of the bodies is s. The densities and r_b/r_a ratio are taken to be the same for the two bodies. The method described in Behrend et al. 2006 was modified to include radar observations. For a circular orbit inclined by an angle ψ from the line of sight, we can deduce directly the separation s when radar observations are made at $\Phi = 0.25$ or 0.75:

$$s = \frac{c\,T}{4\,\pi\,\cos\psi}\,\frac{\Delta\nu}{\nu} \tag{1}$$

The mass M of a body (considered as point-like, for simplicity) can be expressed via the third Kepler law:

$$2\,M = \frac{4\,\pi^2\,s^3}{\mathrm{G}\,T^2} \tag{2}$$

where G is the gravitation constant and T the sideral revolution period. We took sidereal period equal to synodic one because differences are not important for the present study.

From the rotational amplitude Δm, the axis ratio r_b/r_a for prolate ellipsoids can be estimated:

$$\frac{r_b}{r_a} = 10^{-0.4\,\Delta m} \tag{3}$$

Geometrical considerations let us link r_b to s, r_b/r_a and $\Delta\Phi$ (where $\Delta\Phi$ is the duration of a total eclipse relative to the orbital period):

$$r_b = \frac{s/2}{\sqrt{\frac{1}{\tan^2(\pi\,\Delta\Phi)} + \left(\frac{r_b}{r_a}\right)^{-2}}} \tag{4}$$

This formula is exact for prolate bodies even if $r_b \ll s/2$. r_a is deduced from the r_b/r_a ratio. The bulk density ρ is:

$$\rho = \frac{M}{\frac{4}{3}\,\pi\,r_a\,{r_b}^2} \tag{5}$$

Finally, ρ can be rewritten with only measured photometric parameters:

$$\rho = \frac{12\,\pi}{\mathrm{G}}\,\frac{1}{T^2}\,10^{-0.4\,\Delta m}\left(\frac{1}{\tan^2(\pi\,\Delta\Phi)} + 10^{0.8\,\Delta m}\right)^{3/2} \tag{6}$$

Due to the radar observations, s, r_a, r_b are determined without any assumption about absolute magnitude or albedo. Results are presented in the Table 3. Range of values are due to the error propagations in formula 1 to 6 from the input values of Table 1. Initially, ψ is not known. But variations of ψ induce only a linear scaling of the dimensions s, r_a, r_b. Even if ψ is not known, computation of the pole orientation is possible.

Table 3. Ranges of computed parameters of each component of Atami using the model of twin prolate objects using $\psi = 18°$ (see section 3.1 for details).

s **(km)**	**16.07 – 19.03**
r_b/r_b	**0.63 – 0.66**
ρ **(g cm^{-3})**	**2.20 – 3.21**
r_a **(km)**	**2.75 – 3.89**
r_b **(km)**	**1.80 – 2.46**
M **(10^{13}kg)**	**12.5 – 20.9**

The rapid evolution of eclipses suggests the orbital pole is highly inclined to the ecliptic plane. To evaluate this possibility, we built a model based on that described in Kaasalainen & Torppa (2001). That model simulates the reflectance of the binary system including the shadow of one body on the other. We used a Lommel-Seeliger scattering law. We examined trial values of (λ_p, β_p) ecliptic coordinates of the orbital pole at one degree intervals. We obtained the best fit of the model to observations for the solution $\lambda_p = 264 \pm 5°$ and $\beta_p = +5 \pm 5°$ which minimizes the $\Sigma(\Delta e_{obs} - \Delta e_{cal})^2$ parameter at different dates. Usually, light-curves do not allow distinction of prograde or retrograde solution, but in the beginning of 2005 Sep., the phase angle φ was > 20°. This geometry, along with the combination of eclipse and phase effects, provides us the opportunity to determine the pole direction without ambiguity (Fig. 4). With the pole direction estimated, we were able to deduce ψ to be about 18° at time of the radar observations. Results are displayed in Table 3.

Armed with the pole direction, we computed Atami's orientation corresponding to the date 1997 Dec. 21–26 when a C–type reflectance spectrum was obtained (Angeli & Lazzaro 2002). The southern hemisphere was facing the Earth.

A point concerns the amplitude–phase relationship (Zappala et al. 1990) that can reach s(APR)=1.3 10^{-2} deg^{-1} for a S type minor planet observed with a rotational amplitude of 0.476 at a phase angle of 26° (at the date of photometric observations of the Table 1). This effect means that the prolateness is overestimated and the corresponding rotational amplitude, reported at null phase angle, could be only 0.138 mag. The corresponding axis ratio r_b/r_a=0.88 give an upper limit of the prolateness of the bodies. However, the present set observation does not allow to derive the exact value of r_b/r_a. In the case of r_b/r_a=0.88, the bulk density should be 3.3 g cm^{-3} instead of 2.6 g cm^{-3}.

Another point is the biaxial ellipsoid shape assumption that comes from the prediction of mutual tidial effects. From these physical arguements we do not expect the real shape would be very different to a biaxial ellipsoid. However, observations does not constrain the biaxial ellipsoid shape and we could also consider a triaxial ellipsoid. Anyway, the third axis r_c must be lower than r_a. In the later extreme case (r_c=r_a), the bulk density should be 1.7 g cm^{-3} instead of 2.6 g cm^{-3}. On the other hand, if $r_c < r_b$ then the bulk density should be higher than 2.6.

3.2. Albedos

Harris & Lagerros (2002) give an expression to convert the H absolute magnitude to the diameter of a spherical body. We scaled their formula to give the equivalent radius r_{eq} for each body:

$$r_{eq} = 1329\,\mathrm{km}\,\frac{10^{-0.2\,H}}{\sqrt{8\,p}} \tag{7}$$

where p is the geometric albedo. Neglecting some reflectance effects for non spherical bodies, this formula was applied at rotational phase $\Phi = 0.25$ with $r_{eq} = \sqrt{r_a\,r_b}$ and the corresponding brightness $H = 12.67 \pm 0.08$. We derive $p = 0.27 \pm 0.08$. This albedo value lie near the high limit of a S–type. **However, G is unknown (see Section 2.1) and can vary from 0.14 to 0.32 for S–type asteroids. Fortunately the influence of G is not dramatic. We found $p = 0.25 \pm 0.09$, including G and H uncertainties.**

The OC radar cross sections for the two echo spectral peaks (about 2.2 and 3.3 km^2) combined with the model dimensions (see below) and apparent orientation yield an OC radar albedo of about 0.12 for each component. This value is close to the middle of the distributions of values for C and S mainbelt asteroids (Magri et al. 2007). Using the logic described in Magri 2001 and taking into consideration the echo's SC/OC ratio, we find that the smooth part of the asteroid's surface is likely to have a bulk density within about 20% of 2.0 g/cm^3.

3.3. Model 2: two different-sized bodies

Radar observations performed at a ratational phase $\Phi = 0.25$ allows us to derive the mass ratio which is given by:

$$\frac{M_2}{M_1} = -\frac{\nu_1}{\nu_2}. \tag{8}$$

We find $\frac{M_2}{M_1} = 0.55 \pm 0.16$. Assuming the same bulk density for the two bodies, we have also:

$$\frac{r_{eq2}}{r_{eq1}} = \sqrt[3]{-\frac{\nu_1}{\nu_2}} \tag{9}$$

where r_{eq} is the radius for a sphere having the same volume. We find $r_{eq2}/r_{eq1} = 0.82 \pm 0.08$. We verify this ratio is comparable to $\delta\nu_1/\delta\nu_2 = 0.58 \pm 0.17$ - this later determination is not accurate due to the poor S/N of the radar echoes.

We refined our light-curve model to include the ratio r_{eq2}/r_{eq1} just derived as an homothetic factor to values of Table 3. Finally, we plot the simulated light curves in Figures 1 and 4 using the model of two homothetic bodies that fits very well to the observations. **The pole determination (see Section 3.1) is not significantly affected by two non equal size bodies.**

4. Conclusion

This study reveals that Atami is a binary asteroid. Rotation and revolution are synchronous ($T = 27.4466$ h) and the center-to-center separation determined by radar echoes is 17.56 ± 1.48 km. We use a simple model to describe the system: The components are prolate ellipsoids of dimensions ($r_a \times r_b \times r_b$) with the same r_b/r_a ratio. From the flux amplitude outside eclipses we derived $r_b/r_a = 0.65 \pm 0.02$ **but the amplitude–phase relationship is not known and r_b/r_a can reach 0.88** . From the duration of the eclipse features of the light curve, we derive the bulk density $\rho = 2.6 \pm 0.5$ g/cm^3, and the pole orientation: $\lambda_p = 264 \pm 5°$, $\beta_p = +5 \pm 5°$. **These values depend on the model described on Section 3.** The intensity of radar echoes implies that the body dimension ratio is 0.82 ± 0.08. The bulk density is very sensitive to the eclipse duration. As we observed a fast evolution of the eclipse features, this value must be refined during the next oppositions (our model predicts eclipses in 2009, see Fig. 5). Radar albedo and archived spectroscopic observations show that the surface nature is probably moderately rough at decimetre scales. Spectrometry and BVRI photometry performed during eclipses reveal that the two bodies have the same mineralogy and are probably members of the S spectral class. The taxonomic information is inconclusive; higher-quality spectra are needed. Atami should be observed during the next oppositions (Fig. 5). The next radar opportunity as strong as in 2005 occurs in 2035.

Acknowledgements. We thank the A.U.D.E. association support to motivate new members and to communicate quickly between observers. Some of this work was performed at the Jet Propulsion Laboratory (JPL), California Institute of Technology, under contract with NASA. This material is based in part on work supported by the Science Mission Directorate Research and Analysis Programs. The Arecibo Observatory is part of the National Astronomy and Ionosphere Center, which is operated by Cornell University under a cooperative agreement with the National Science Foundation.

References

Angeli, C.A. & Lazzaro D., 2002, A&A 391, 757
Behrend, R., Roy, R., Bernasconi, L., et al. 2006, A&A 446, 1177
Bus, S., Binzel, R., 2002, Icarus 158, 106
Bus, S., Binzel, R., 2002, Icarus 158, 146
Danby, J., in Fundamentals of celestial mechanisms 1992, ed. Willmann-Bell
Harris, A.W & Lagerros, J.S.V. 2002, in Asteroids III, ed. W.F. Bottke, A. Cellino, P. Paolicchi, & R.P. Binzel (Univ. of Arizona), 205-218
Kaasalainen, M. & Torppa J., 2001, Icarus 153, 24
Klotz, A. et al. 2005, A&A 439, L35
Goncalves, R., Coloma, J., Behrend, R., 2005, CdR&CdL website, http://obswww.unige.ch/~behrend/page_cou.html
Høg, E., Fabricius, C., Makarov, V. V., et al., 2000, Guide to the Tycho-2 Catalog
Lemaitre, G. et al. 1990, A&A 228, 546

Lupishko, D. F., Velichko, F. P., Shevchenko, V. G. 1988 Astronomicheskii Vestnik 22, 167
Manzini et al., 2006, CBET 430, 1
Magri, C., Consolmagno, G. J., Ostro, S. J., Benner, L. A. M. and Beeney, B. R., 2001, Meteoritics Planet. Sci. 36, 1697-1709
Magri, C., Nolan, M. C., Ostro, S. J. and Giorgini, J. D., 2007, Icarus 186, 126-151
Margot, J.-L., Nolan, M. C., Negron, V. et al., 2003, IAUC 8227.
Merline, W.J., Close L.M., Shelton, J.C. et al., 2000, IAUC 7503
Merline, W.J., Close L.M., Siegler, N., 2001, IAUC 7741
Migliorini A., Zappalà, V., Cellino, A., 1998, Icarus 118, 271
Michel, P., Migliorini A., Zappalà, V., 2000 Icarus 145, 332
Michel, P., Benz, W. , Tanga, P., Richardson, D.C., 2001 Science 294, 1696
Michalowski, T., Bartczak, P., Velichko, F. P., et al., 2004, A&A 423, 1159
Pravec, P., Hahn, G., 1997, Icarus 127, 431
Pravec, P., Sarounová, L., Rabinowitz, D.L. et al., 2000, Icarus 146, 190
Pray, D. P., P. Pravec, P. Kusnirak et al., 2006, CBET 328
Pray, D. P., P. Pravec, P. Kusnirak et al., 2006, CBET 353
Tedesco, E. F., Williams, J. G., Matson, D. L. et al., 1989, AJ 97, 580
Veillet, C., Parker, J.Wm., Griffin, I., 2002, Nature 416, 711
Warner, B. D., Pray, D., Pravec, P. et al., 2005, CBET 341
Zappalà, V., Cellino, A., Barucci, A.M., et al., 1990, A&A 231, 548

[1] Observatoire de Genève, CH–1290 Sauverny, Switzerland
[2] Stazione Astronomica di Sozzago, I–28060 Sozzago, Italy
[3] CESR, Obseratoire Midi-Pyrénées, CNRS-UPS, BP 4346, F–31028 Toulouse Cedex 04, France
[4] Observatoire de Haute Provence, F–04870 Saint Michel l'Observatoire, France
[5] IMCCE, 77 avenue Denfert–Rochereau, F–75014 Paris, France
[6] Association des Utilisateurs de Détecteurs Electroniques (A.U.D.E.), France
[7] Jet Propulsion Laboratory, California Institute of Technology, Pasadena, CA 91109-8099, USA
[8] Observatoire de Bédoin, 47 rue Guillaume Puy, F–84000 Avignon, France
[9] Observatoire des Engarouines, F–84570 Mallemort-du-Comtat, France
[10] 49 rue des Glycines. F–49430 Durtal, France
[11] Agrupación Astronómica de Sabadell, P.O. Box 50, E–08200 Sabadell, Spain
[12] 11 rue du Puits Coellier, FR–37550 Saint-Avertin, France
[13] 980 Antelope Drive West, Bennett, CO 80102 USA
[14] Chante Perdrix, Dauban, F–04150 Banon, France
[15] Arecibo Observatory, HC3 Box 53995, Arecibo, PR 00612, USA
[16] Association T60, 14 Avenue Edouard Belin, F–31400 Toulouse, France
[17] 66 cours de Lassus, F–66000 Perpignan, France
[18] University of Maine at Farmington, 173 High Street – Preble Hall, Farmington, ME–04938, USA
[19] Department of Astronomy, Space Sciences Building, Cornell University, Ithaca, NY–14853-6801, USA
[20] Nyrölä Observatory, Jyväskylän Sirius ry, Kyllikinkatu 1, FI–40100 Jyväskylä, Finland
[21] Jakokoski Observatory, University of Joensuu, P.O. Box 111, FI-80101 Joensuu, Finland
[22] 2 Rue des Ecoles, F–34920, Le Crès, France
[23] Observatoire de Blauvac, F–84570 St-Estève, France
[24] DeKalb Observatory, 2507 CR 60, Auburn, IN–46706, USA
[25] Centre d'astronomie de Saint Michel l'Observatoire, F–04870 Saint Michel l'Observatoire, France
[26] Institut de physique, Université de Neuchâtel, CH–2000 Neuchâtel, Switzerland

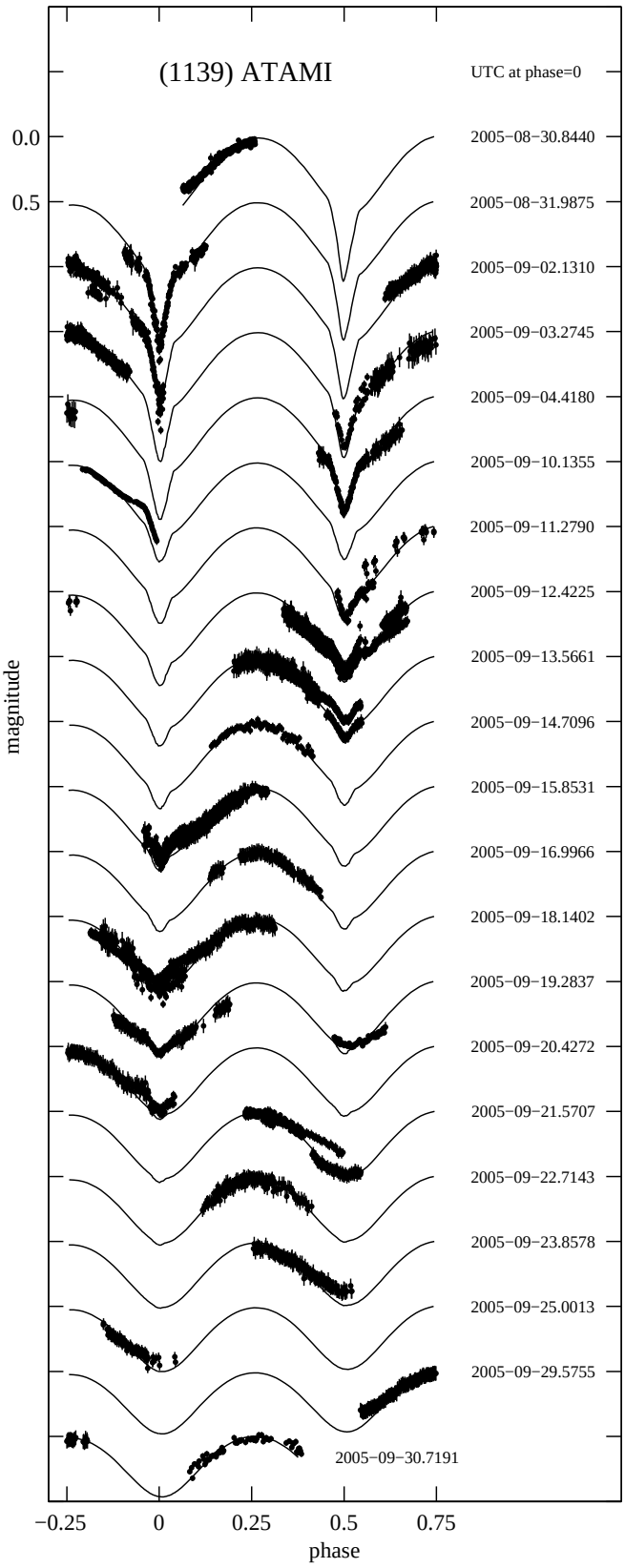

Fig. 1. Phased light curves for all observations of Atami from data of its study assuming a period of 27.384 hours. Observations are black dots. Thin curves are come from the model described in the text (λ_p = 264°, β_p = +5°). Each curve is shifted by 0.5 magnitude and normalized to zero magnitude for the brightest part.

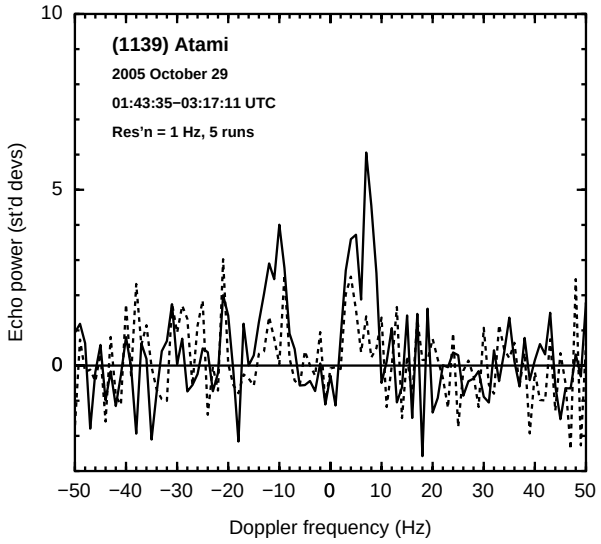

Fig. 2. Arecibo radar echoes from Atami. Continuous curve: OC sense of polarization. Dashed curve: SC sense of polarization (see text).

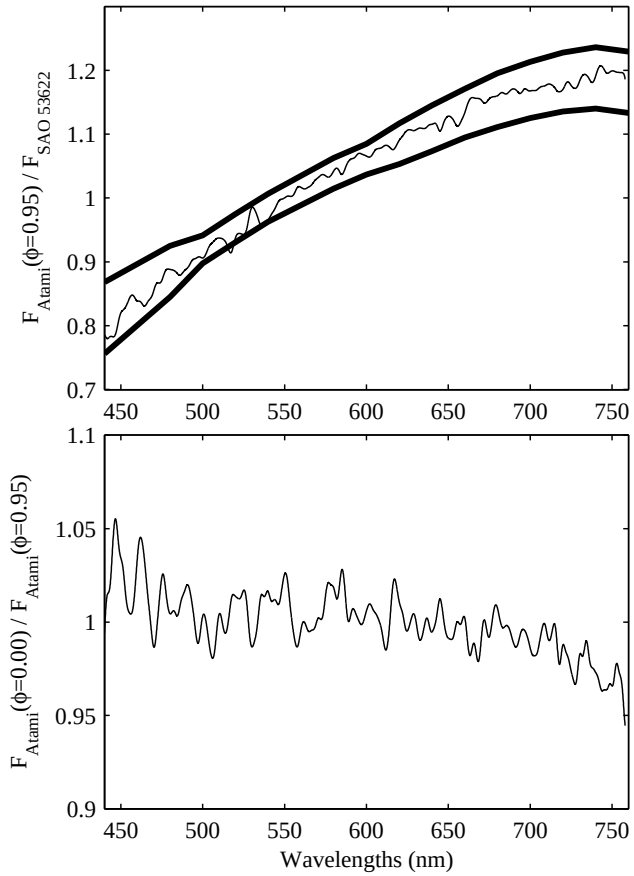

Fig. 3. Top: reflectance spectrum of Atami. Thick curves locate the limiting reflectance at 2 σ for S–type asteroids from Bus & Binzel (2002b). Bottom: Ratio of the two spectra of Atami taken at phases 0.00 (total eclipse) and 0.95 (just outside eclipse).

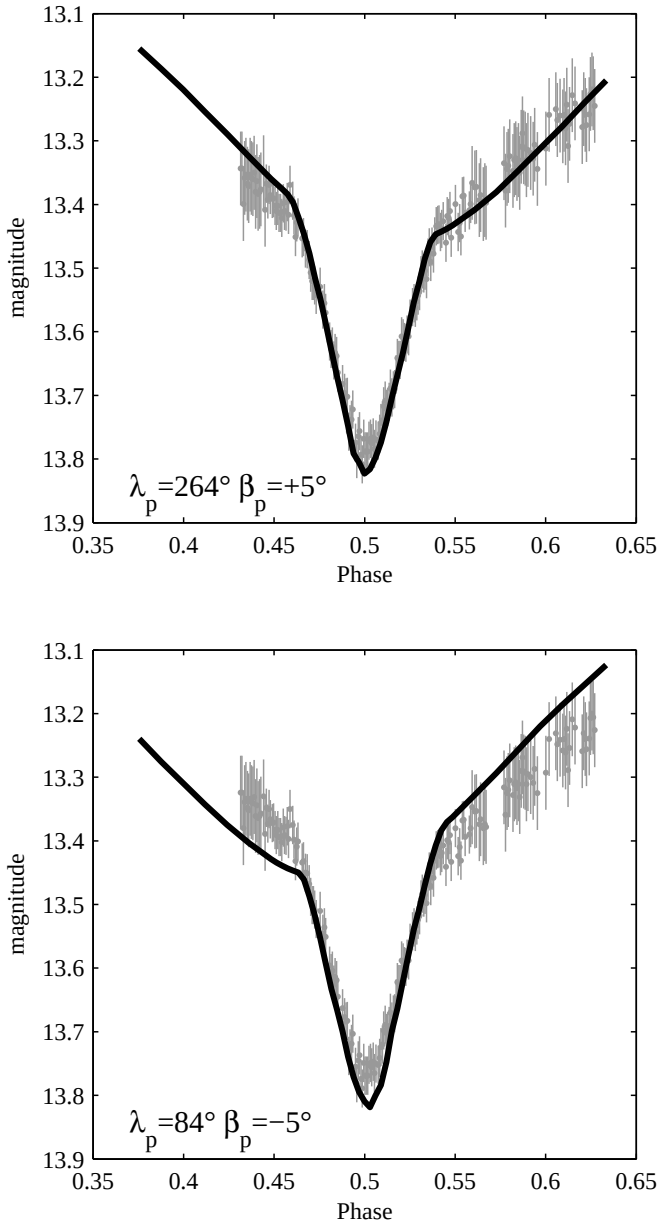

Fig. 4. Phased light curve measurements (gray lines) centered on the eclipse that occurred in 2005 Sep. 4.990 UT. The black lines are magnitudes computed by the model described in the text. The phase effect permitted unambiguous estimation of the pole direction.

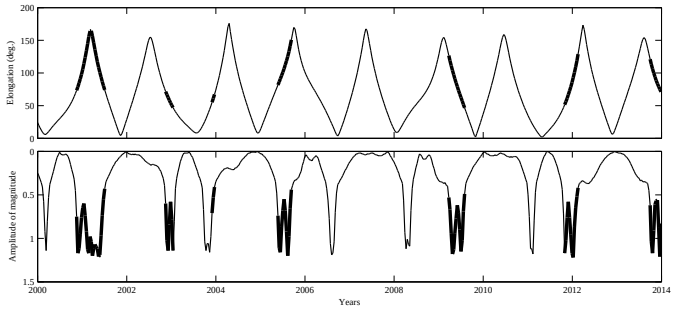

Fig. 5. Top: Elongation of Atami as seen from Earth. Bottom : Amplitude of magnitude during one period. Bold parts correspond to best windows to study mutual events of Atami (elongations greater than 50° and amplitudes greater than 0.5 magnitude).